ADVANCED FUNCTIONAL MATERIALS
www.afm-journal.de

www.MaterialsViews.com

Well-Defined Functional Linear Aliphatic Diblock Copolyethers: A Versatile Linear Aliphatic Polyether Platform for Selective Functionalizations and Various Nanostructures

Wonsang Kwon, Yecheol Rho, Kensuke Kamoshida, Kyung Ho Kwon, Youn Cheol Jeong, Jonghyun Kim, Hideki Misaka, Tae Joo Shin, Jehan Kim, Kwang-Woo Kim, Kyeong Sik Jin, Taihyun Chang, Heesoo Kim, Toshifumi Satoh, Toyoji Kakuchi,* and Moonhor Ree**

Low-temperature anionic ring-opening homopolymerizations and copolymerizations of two glycidol derivatives (allyl glycidyl ether (AGE) and ethoxyethyl glycidyl ether (EEGE)) are studied using a metal-free catalyst system, 3-phenyl-1-propanol (PPA) (an initiator) and 1-*tert*-butyl-4,4,4-tris(dimethylamino)-2,2-bis[tris-(dimethylamino) phosphoranylidenamino]-2Λ^5,4Λ^5-catenadi(phosphazene) (*t*-Bu-P_4) (a promoter) in order to obtain well-defined functional linear polyethers and diblock copolymers. With the aid of the catalyst system, AGE is found to successfully undergo anionic ring-opening polymerization (ROP) even at room temperature (low reaction temperature) without any side reactions, producing well-defined linear AGE-homopolymer in a unimodal narrow molecular weight distribution. Under the same conditions, EEGE also undergoes polymerization, producing a linear EEGE-homopolymer in a unimodal narrow molecular-weight distribution. In this case, however, a side reaction (i.e., chain-transfer reaction) is found to occur at low levels during the early stages of polymerization. The chemical properties of the monomers in the context of the homopolymerization reactions are considered in the design of a protocol used to synthesize well-defined linear diblock copolyethers with a variety of compositions. The approach, anionic polymerization via the sequential step feed of AGE and EEGE as the first and second monomers, is found to be free from side reactions at room temperature. Each block of the obtained linear diblock copolymers undergoes selective deprotection to permit further chemical modification for selective functionalization. In addition, thermal properties and structures of the polymers and their post-modification products are examined. Overall, this study demonstrates that a low-temperature metal-free anionic ROP using the PPA/*t*-Bu-P_4 catalyst system is suitable for the production of well-defined linear AGE-homopolymers and their diblock copolymers with the EEGE monomer, which are versatile and selectively functionalizable linear aliphatic polyether platforms for a variety of post-modifications, nanostructures, and their applications.

1. Introduction

Poly(ethylene glycol) (PEG) has a low toxicity, immunogenicity, and antigenicity. PEG has been used widely as a biocompatible polymer in a broad range of biomedical and pharmaceutical applications.[1] Despite its advantageous properties, the use of PEG is often limited by its low functional group loading capacity.[1]

One strategy for improving the functionality of PEG is to synthesize linear glycidol polymers and their derivatives because these monomers introduce numerous end functional groups into the PEG backbone.[2] Significant research has been conducted toward the goal of polymerizing glycidol and its derivatives.[3–5] As a result, anionic and coordination polymerization methods have been developed for the production of linear glycidol polymers and their derivatives.[3–5] The coordinated polymerization approach, aided through the use of diethylzinc or a calcium amide alkoxide catalyst, was reported to give a high molecular weight polyglycidol; however, the polyether was in multimodal and/or high polydispersity index (PDI).[3] In comparison, anionic ring-opening

W. Kwon, Y. Rho, K. H. Kwon, Y. C. Jeong, J. Kim, Prof. T. Chang, Prof. M. Ree
Department of Chemistry
Division of Advanced Materials Science
Pohang Accelerator Laboratory
Center for Electro-Photo Behaviors in Advanced, Molecular Systems
Polymer Research Institute, and BK School of Molecular Science
Pohang University of Science and Technology
Pohang 790-784, Republic of Korea
E-mail: ree@postech.edu

K. Kamoshida, H. Misaka, Prof. T. Satoh, Prof. T. Kakuchi
Polymer Chemistry Laboratory
Division of Biotechnology and Macromolecular Chemistry
Faculty of Engineering
Hokkaido University
Sapporo 060-8628, Japan
E-mail: satoh@poly-bm.eng.hokudai.ac.jp; kakuchi@poly-bm.eng.hokudai.ac.jp

J. Kim, Dr. T. J. Shin, Dr. K.-W. Kim, Dr. K. S. Jin
SAXS Group, Beamline Division
Pohang Light Source-II (PLS-II)
Pohang Accelerator Laboratory
Pohang University of Science and Technology
Pohang 790-784, Republic of Korea

Prof. H. Kim
Dongguk University College of Medicine and Dongguk Medical Institute
Gyeongju 780-714, Republic of Korea

DOI: 10.1002/adfm.201201101

polymerization (ROP) approaches using alkali metal alkoxide initiators can produce polyglycidol and its derivatives with unimodal and low PDI values.[4,5] In general, polymers with lower PDI value and more homogeneous composition have been known to exhibit a narrower interface, larger structural size and a sharper morphological transition, compared to the corresponding polymers with high PDI value.[6] For example, in case of the drug delivery with the aid of a polymer the PDI value was reported to influence the polymer degradation as well as the drug release rate.[7] The anionic polymerization approach is, therefore, generally considered to be better than the coordination polymerization approach.

However, anionic ROP approach can suffer from certain drawbacks.[5,8–11] Anionic polymerization can produce relatively low molecular weight polymer products, sometimes very low molecular weight products, compared to coordination polymerization approaches. Anionic polymerization requires the hydroxyl groups in the glycidol monomers to be protected before the reaction may proceed; otherwise, the unprotected glycidol monomer leads to a highly branched structure in the polymer product. Examples of suitable protecting groups are the allyl ether group, as in the allyl glycidyl ether, and the acetal group, as in the ethoxyethyl glycidyl ether. Competitive side reactions, such as chain transfer to the monomer or chain termination, often reduce the yield in anionic polymerization reactions, thereby limiting the production of high molecular weight products with a unimodal distribution.[10,11] Such side reactions were also observed for the polymerizations of alkylene oxides.[12] The undesired side reaction issues may be mitigated by lowering the reaction temperature and/or the metal content in the alkali metal alkoxide catalyst systems; however, the side reactions could not be eliminated completely.[10–13] Thus, anionic ROP of glycidol and its derivatives, which can produce polymer products with unimodal distributions free from side reactions, are still under exploration.

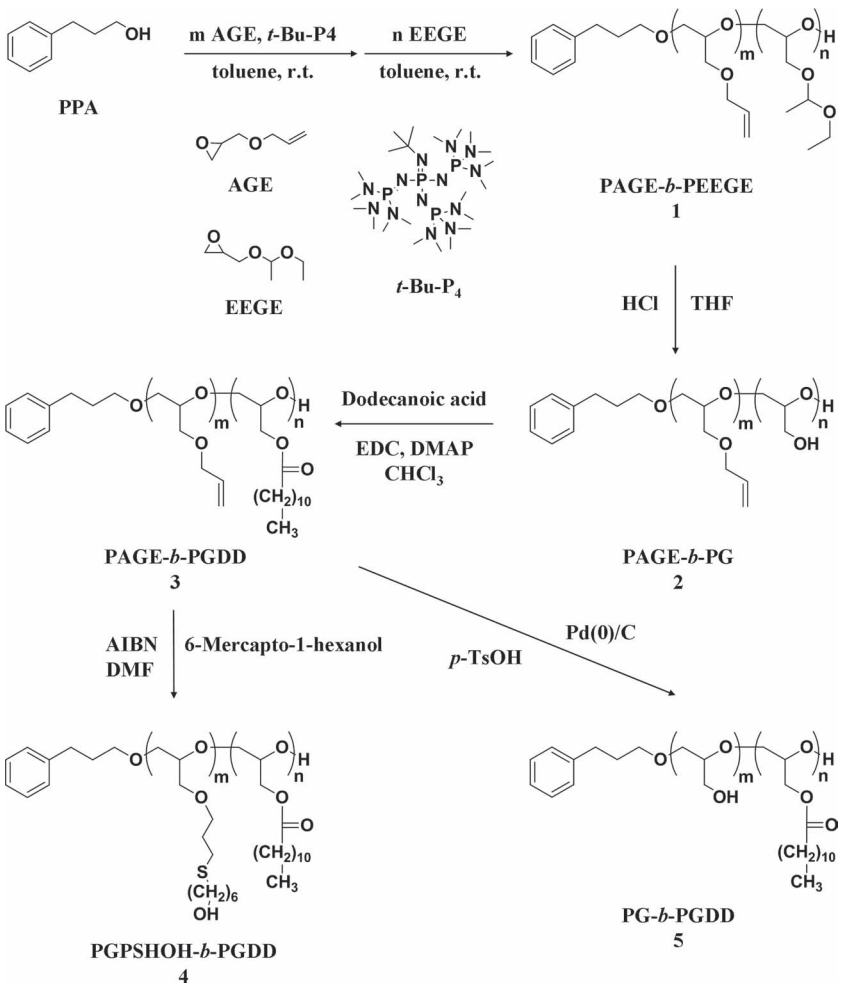

Scheme 1. Synthesis of poly(allyl glycidyl ether-*block*-ethoxyethyl glycidyl ether) (PAGE-*b*-PEEGE) by low temperature (i.e., room temperature) anionic ring-opening polymerization with the aid of PPA/*t*-Bu-P_4 catalyst system, and the resulting diblock copolymers' selective deprotections and functionalizations.

In this study, we report the synthesis of well-controlled functionalized linear aliphatic diblock copolyethers from allyl glycidyl ether (AGE) and ethoxyethyl glycidyl ether (EEGE) via room-temperature metal-free anionic ROP with the aid of a catalyst system, 3-phenyl-1-propanol (PPA; an initiator) and 1-*tert*-butyl-4,4,4-tris(dimethylamino)-2,2-bis[tris(dimethylamino) phosphoranylidenamino]-2Λ^5,4Λ^5-catenadi(phosphazene) (*t*-Bu-P_4; a promoter) (**Scheme 1**). Anionic polymerizations of the AGE monomer were successfully demonstrated without side reactions over a range of monomer feed ratios in the catalyst system, producing the homopolymer products with a unimodal narrow molecular weight distribution. In contrast, chain transfer reactions during anionic polymerization of the EEGE monomer could be suppressed significantly but could not be eliminated completely. However, the side reactions (which were observed in the polymerization of EEGE) were completely eliminated in the sequential anionic polymerization of AGE and EEGE, providing well-defined linear diblock copolyether products with a unimodal molecular weight distribution. The obtained linear diblock copolyethers were confirmed to undergo selectively deprotection reaction in each block and further post chemical modification for selective functionalization. Moreover, the diblock copolymers nicely demonstrated various nanostructures via favorable phase-separation and molecular ordering, depending on the compositions and selective post-functionalizations.

2. Results and Discussion

We attempted to synthesize well-defined linear aliphatic homopolyethers and diblock copolyethers from AGE and EEGE by anionic ROP. To overcome the severe drawbacks observed using common alkali metal alkoxide catalysts, in this study we

Table 1. Anionic ring-opening homopolymerization of AGE and EEGE monomers in toluene using the PPA/*t*-Bu-P_4 catalyst system. Temperature: rt.; $[M]_0 = 3$ M; $[t\text{-Bu-P4}]_0/[PPA]_0 = 1$.

Entry No.	Monomer	$[M]_0/[PPA]_0$	Conversion (%)	$M_{n,theo}$ [a] [g/mol]	$M_{n,nmr}$ [b] [g/mol]	$M_{n,sec}$ [c] [g/mol]	M_w/M_n [c]
1	AGE	20	95	2420	2300	2890	1.10
2	AGE	40	≥99	4700	5040	6820	1.11
3	AGE	60	≥99	6985	7210	8950	1.08
4	AGE	80	99	9268	9150	9210	1.14
5	EEGE	20	≥99	3060	3205	4840	1.14
6	EEGE	40	97	5980	5810	5430	1.15
7	EEGE	60	98	8910	8745	9090	1.14
8	EEGE	80	94	11 830	11 100	10 230	1.14

[a]Molecular weight calculated based on the conversion and the monomer to initiator ratio; [b]Molecular weight determined by ^{1}H NMR analysis; [c]Molecular weights determined by SEC in THF using PS standards; here M_n and M_w denote the number- and weight-averaged molecular weights respectively.

attempted to achieve low-temperature anionic ROPs using a metal-free catalyst system, PPA/*t*-Bu-P_4.

The sequential block copolymerization of the two protected glycidol monomers was carried out by the homopolymerization of each monomer using a set of monomer feed ratios in the initiator system. The homopolymerization results are summarized in **Table 1**. For all reactions, the conversions of both EEGE and AGE monomers exceeded 94% or higher after 20 h. Here, the conversions were determined from the proton (^{1}H) nuclear magnetic resonance (NMR) spectra by end group analysis based on the methylene proton of the initiator and the allyl and ethoxyethyl protons of the monomers. For the obtained PAGE and PEEGE homopolymers, the experimental $M_{n,nmr}$ values were found to be almost equal to the theoretical values. The PDI was relatively low (1.08 – 1.15), indicating that the polymerization occurred in a living fashion. The results collectively indicate that the PPA/*t*-Bu-P_4 catalyst system is suitable for homopolymerizations of the protected glycidol monomers and also for their block copolymerizations.

To understand the characteristics of the homopolymerization reactions, including possible side reactions, the homopolymer products were further analyzed quantitatively. For the PAGE products, the size exclusion chromatography (SEC) analysis showed a sharp, unimodal peak in the molecular weight distribution, yielding a low PDI value (**Figure 1**). The SEC traces of the PAGE products, which were monitored using a refractive index (RI) detector, provided almost the same peak shapes and retention times as the ultraviolet (UV) detector (Figure S1, Supporting Information), indicating that the PPA initiator was linked to the PAGE chains.

The NMR spectra indicated the absence of side reactions (see the ^{1}H NMR spectra in **Figure 2**a and the ^{13}C NMR spectra in Figure S2a, Supporting Information). The matrix-assisted laser desorption/ionization time-of-flight (MALDI-TOF) mass spectra gave more direct evidence for the polymer chemical structure. **Figure 3** shows typical MALDI-TOF mass spectrum for one of the obtained PAGE homopolymers. The mass spectrum displayed one series of peaks in regular intervals of 114, corresponding to the molar mass of the AGE monomer unit. The peak at m/z = 5063.7 corresponded to the 43-mer of the AGE homopolymer initiated from the PPA initiator. Thus, the series of peaks were assigned to the AGE homopolymer chemical structure having a 3-phenylpropoxyl group (originating from the initiator) at one chain end and a hydroxyl group at the other chain end. This analysis collectively confirms that the ROP of AGE with the aid of PPA/*t*-Bu-P_4 system proceeded in a living manner without side reactions, such as isomerization, chain transfer, or chain termination reactions. This homopolymerization without side reactions is remarkable in view of common anionic polymerization reactions that use alkali metal alkoxide initiators and are accompanied with chain transfer and termination reactions[10,11,14] or isomerizations of allyl repeat units.[15,16]

The SEC spectra of the PEEGE homopolymers revealed a unimodal molecular weight distribution peak with a low PDI.

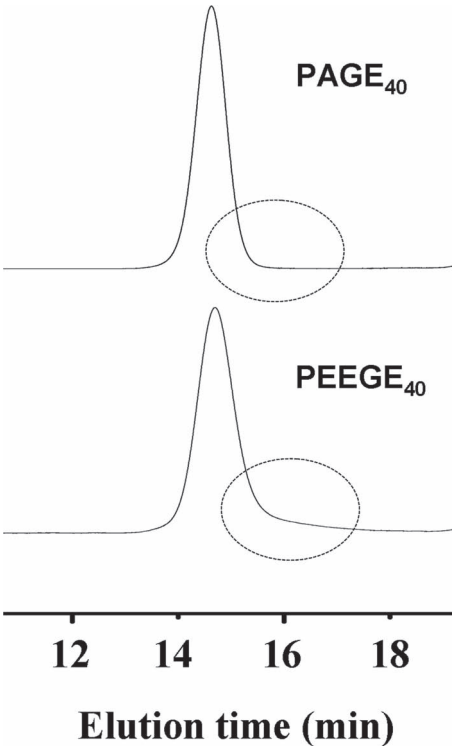

Figure 1. SEC chromatographs of two homopolymers: PAGE (Table 1, Entry 2) and PEEGE (Table 1, Entry 6).

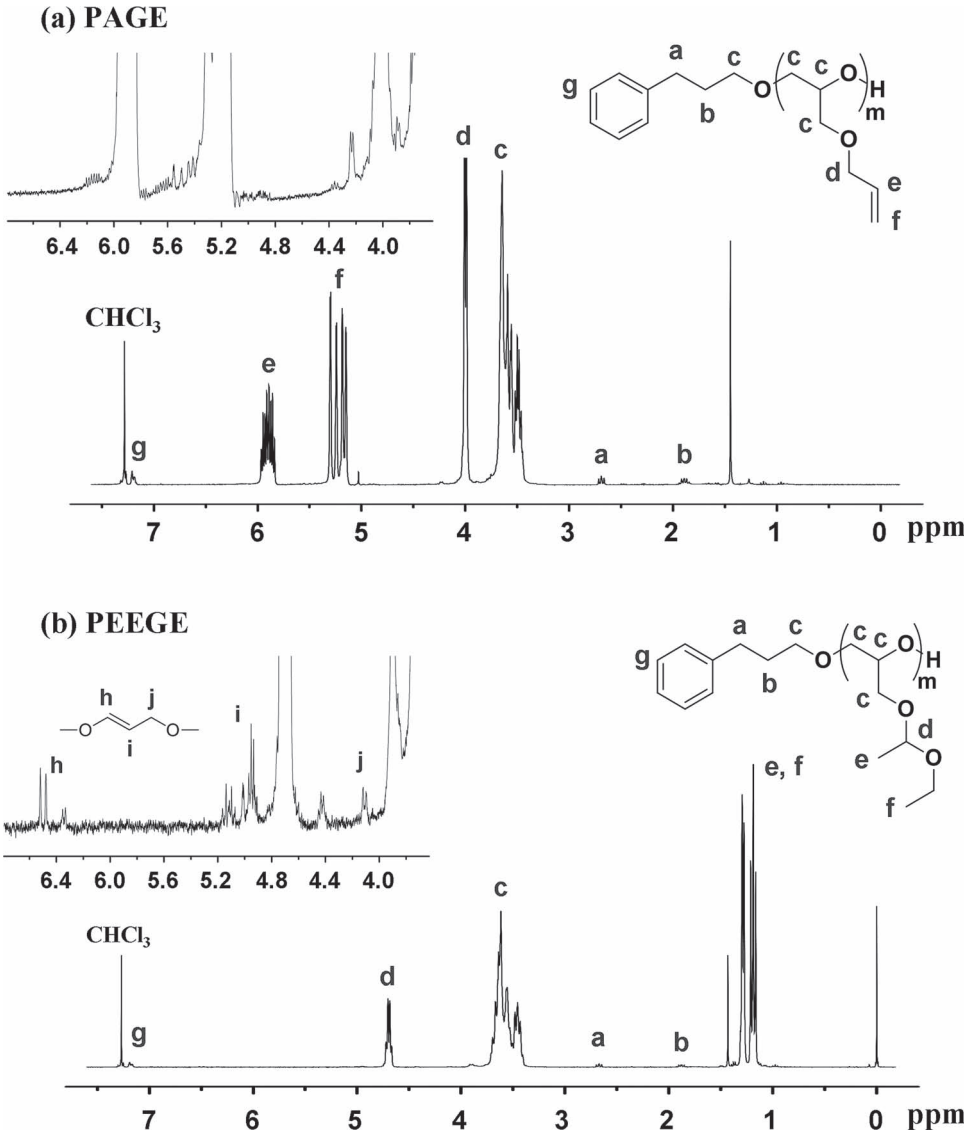

Figure 2. ^{1}H NMR spectra of: a) PAGE (Table 1, Entry 2) and b) PEEGE (Table 1, Entry 6) in $CDCl_3$. Each inset shows the expanded spectrum of the 3.6–6.8 ppm region.

The very weak tail of this peak toward longer elution times (Figure 1) indicated the presence of low molecular weight products in small amounts. On the other hand, the ^{1}H NMR spectra revealed the presence of weak allylic ether protons in the range 4.1–6.5 ppm (Figure 2b), indicating that allylic ether units were generated by unfavorable chain transfer reactions during homopolymerization of EEGE. The allylic carbons could not be detected in the ^{13}C NMR analysis (Figure S2b, Supporting Information) due to the poor detection limit compared to ^{1}H NMR spectroscopy. These NMR results confirmed that the side reaction proceeded to a small extent during the anionic polymerization. The small amounts of side reaction products were clearly detected by MALDI-TOF mass analysis. The mass spectrum revealed two rather than one series of peaks (**Figure 4**). The peaks in one high molecular weight series were separated by regular molar mass intervals of 146.09, corresponding to the EEGE monomer unit. The PEEGE homopolymer structure included a 3-phenylpropoxyl group at one chain end and a hydroxyl group at the other chain end, yielding the sum 146.09 (EEGE unit) × n (number of monomer unit) + 135.08 (one 3-phenylpropoxyl initiator) + 23 (Na ion salt) + 1.01 (one terminal H). The other series of peaks appeared in the relatively low molecular weight region and displayed an intensity much weaker than the peak intensity observed in the high molecular weight region. This indicates that the low molecular weight polymers were present in minor quantities. In the overlapping regions of the major and minor sets of mass peaks, each peak in the minor set was clearly shifted toward larger masses by 10 Dalton (Da) relative to the corresponding peak in the major set. This mass difference was equal to the difference between the 3-phenylpropoxyl group (originating from the initiator) and the allylic alkoxide group (generated by the chain transfer reaction to the EEGE monomer) (**Scheme 2**). Overall, these results indicate that the chain transfer reaction occurred

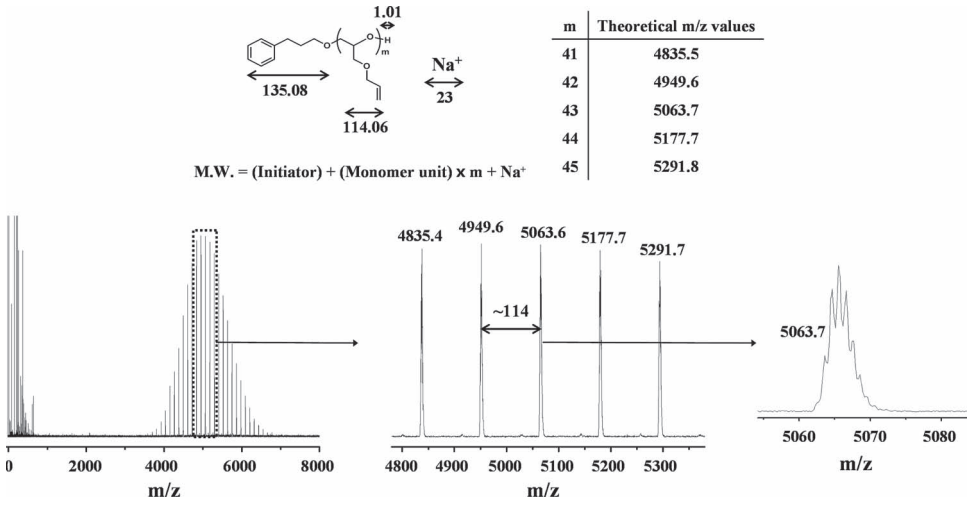

Figure 3. MALDI-TOF mass spectrum of PAGE (Table 1, Entry 2).

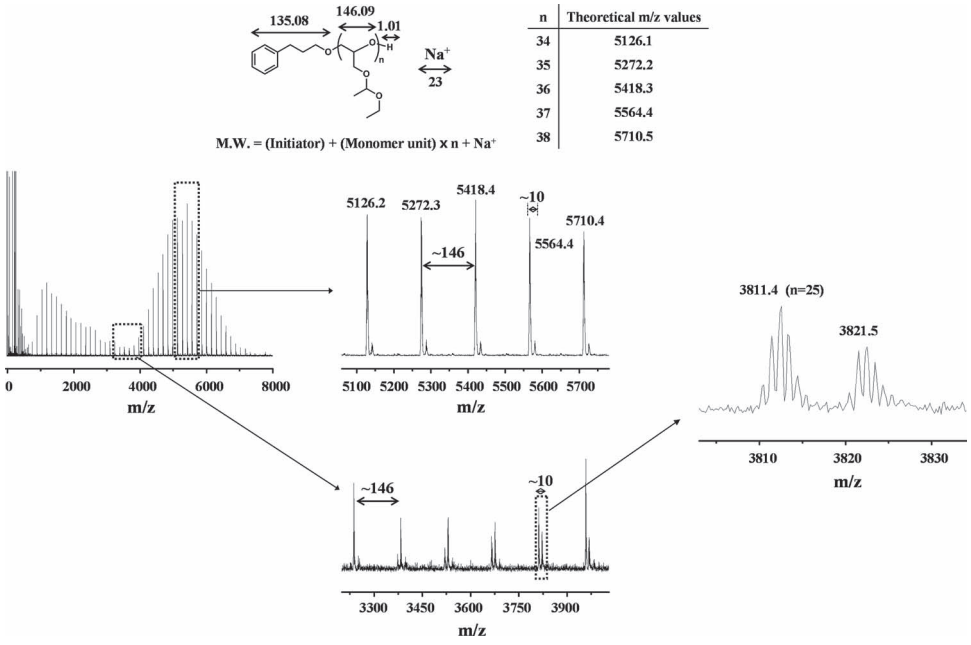

Figure 4. MALDI-TOF mass spectrum of PEEGE (Table 1, Entry 6).

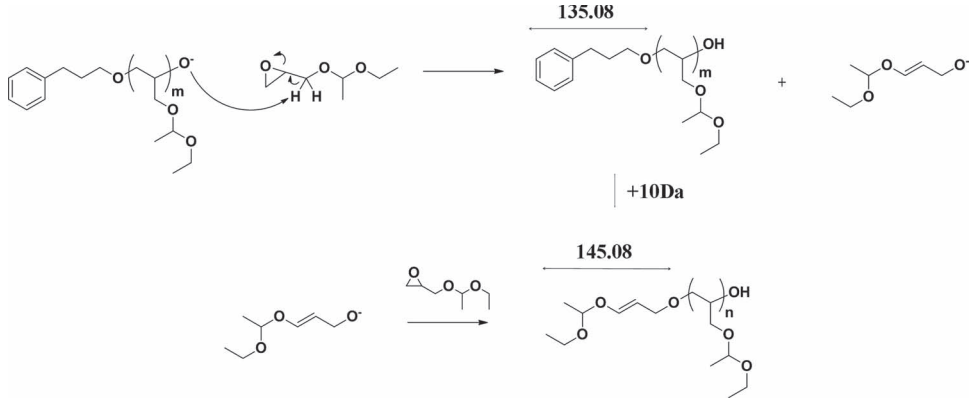

Scheme 2. Mechanism of the chain transfer to the EEGE monomer in the room-temperature anionic ring-opening polymerization with the aid of the PPA/*t*-Bu-P_4 catalyst system.

mainly during the early stages of polymerization rather than the propagation stage. The side reaction in the EEGE homopolymerization was significantly suppressed compared to the side reactions observed during anionic polymerizations with alkali metal alkoxide initiator systems.[10,11,16]

The chain transfer reaction in the anionic polymerization of the protected glycidol monomers may begin with the abstraction of a methylene proton adjacent to the epoxide ring by the active alkoxide chain end (Scheme 2). As a result, the allylic alkoxide is generated and initiates polymerization, leading to byproduct polymers (Scheme 2). Such chain transfer reactions depend on the basicity of the alkoxide chain end as well as the acidity (i.e., reactivity) of the methylene protons adjacent to the epoxide ring of the protected glycidyl monomers.[11,12]

As discussed above, no chain transfer reaction was detected in the AGE polymerization. This result may be explained as follows. The polymerization was carried out at low temperatures (i.e., room temperature). The *t*-Bu-P_4 promoter is a very strong base (pK_a = 30.2 in dimethylsulfoxide)[17] and can act as a soft counter ion compared to the metal counter ions in the alkali metal alkoxide initiator systems. Furthermore, the promoter is bulky and imposes steric hindrance that reduces the reactivity of the PPA initiator. In the protected glycidol monomers, the epoxide ring methylene protons experience less sterically hindered environments compared to the methylene protons adjacent to the epoxide ring. These three factors could conspire during the initiation step to increase the selectivity of the PPA initiator' nucleophilic attack for the epoxy ring, rather than the methylene protons adjacent to the epoxide ring in the AGE monomer. During the propagation step, the bulky promoter may also enhance the selectivity of the living alkoxide chain during nucleophilic attack on the epoxide ring of the monomer. In the living alkoxide chain, the long chain causes additional steric hindrance and could, thus, contribute positively toward enhancing the selectivity in the nucleophilic attack on the epoxide ring of the monomer. On the other hand, the acidity of the methylene protons adjacent to the epoxide ring in the AGE monomer may not be high enough to allow the attack of the PPA initiator and the living alkoxide chain.

A small portion of the chain transfer reaction was observed during the early stages of the EEGE polymerization. This result suggests that the reactivity of the methylene protons adjacent to the epoxide ring in the EEGE monomer was not weak enough to prevent the attack of the PPA initiator. The protecting groups of both the EEGE and AGE monomers included oxygen, carbon, and hydrogen atoms. The electronegativity of oxygen is larger than the electronegativities of carbon and hydrogen, and the vinyl unit is weakly electron-donating. Overall, the ethoxyethyl protecting group may display a stronger electron pull than the allyl protecting group. The difference between the electron-withdrawing strengths of the protecting groups render the methylene protons adjacent to the epoxide ring in the EEGE monomer more acidic than those in the AGE monomer. Thus, the observed chain transfer reaction was attributed to the relatively high acidity of the methylene protons adjacent to the epoxide ring in the EEGE monomer. The acidity was very limited and indeed permitted a small amount of chain transfer reaction. In fact, the ethoxyethyl protecting group was bulkier than the allyl group. Thus, the bulkier ethoxyethyl group could severely limit nucleophilic attack of the PPA initiator, in the presence of the very bulky *t*-Bu-P_4 counter ion, on the methylene protons adjacent to the epoxide ring. Moreover, in the presence of the *t*-Bu-P_4 counter ion, nucleophilic attack by the living chain alkoxide with high bulkiness on the methylene protons adjacent to the epoxide ring could be completely blocked due to steric hindrance. In addition, the reactivity of the active species generated by PPA and *t*-Bu-P_4 in the initiation step might be relatively higher than that of the propagating living chain alkoxide. Thus, the relatively higher active species lead to the side reaction in the early stage of EEGE polymerization.

The metal-free low-temperature anionic polymerization reaction described above was extended to diblock copolymerization of the AGE and EEGE monomers. As discussed, unfavorable side reactions were observed in limited amounts during the early stages of EEGE homopolymerization; however, such side reactions were prevented in the propagation step. No side reactions were observed in the AGE homopolymerization. These results supported the selection of AGE and EEGE as the first and second monomers, respectively, to be fed sequentially during anionic diblock copolymerization. The diblock copolymerization results are summarized in **Table 2**.

The conversions of the first and second monomers in all diblock copolymerizations were found to be ≥99.9% and ≥97% respectively by NMR spectroscopy (**Figure 5**). NMR spectroscopy analysis indicated no evidence for side reaction for any of the diblock copolyether products obtained using various compositions (Figure 5). The experimental $M_{n,nmr}$ value of each block was found to be very close to the theoretical value (Table 2). **Figure 6** shows typical SEC chromatograms measured for the AGE block (sampled immediately after completing

Table 2. Anionic ring-opening diblock copolymerization of AGE and EEGE monomers in toluene using the PPA/*t*-Bu-P_4 catalyst system. Room temperature; $[M_1]_0$ = 3 M; $[M_2]_0$ = 2 M; [t-Bu-P4]$_0$/$[PPA]_0$ = 1.

Entry No.	AGE [a]/EEGE[b]	$M_{n,theo}$[c] (g/mol)		$M_{n,nmr}$[d] (g/mol)		$M_{n,sec}$[e] (g/mol)	M_w/M_n[e]
		1st block	2nd block	1st block (DP)	2nd block (DP)		
1	20/60	2420	8770	2190(18)	8910(60)	11700	1.11
2	40/40	4700	5850	4587(39)	5980(40)	9800	1.15
3	60/20	6985	2925	6985(60)	2913(19)	12200	1.13

[a]$[M_1]_0/[PPA]_0$ ratio; [b]$[M_2]_0/[PPA]_0$ ratio; [c]Molecular weight calculated based on the conversion and the monomer to initiator ratio; [d]Molecular weight determined by ^{1}H NMR analysis; [e]Molecular weights determined by SEC in THF using PS standards; here M_n and M_w denote the number- and weight-averaged molecular weights respectively.

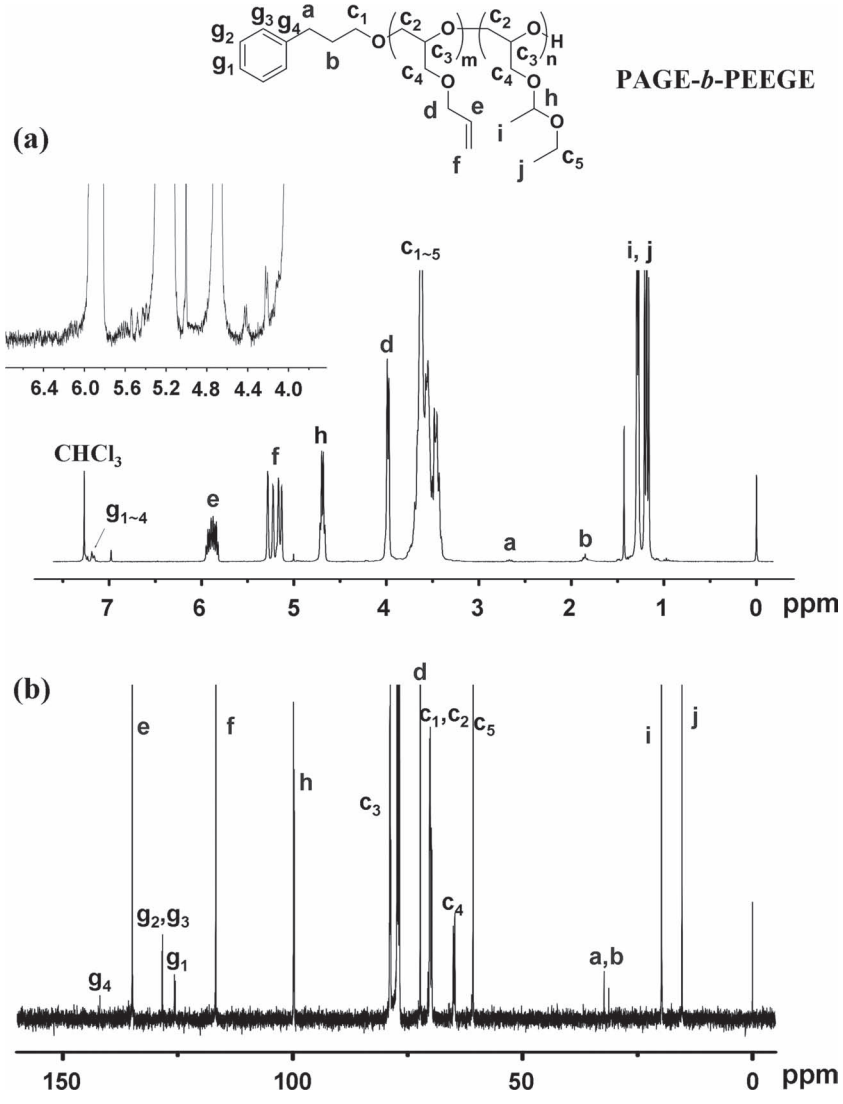

Figure 5. (a) ^{1}H and (b) ^{13}C NMR spectra of $PAGE_{40}$-*b*-$PEEGE_{40}$ (Table 2, entry 2) in $CDCl_3$. The inset shows the expanded spectrum of the 3.6–6.8 ppm region.

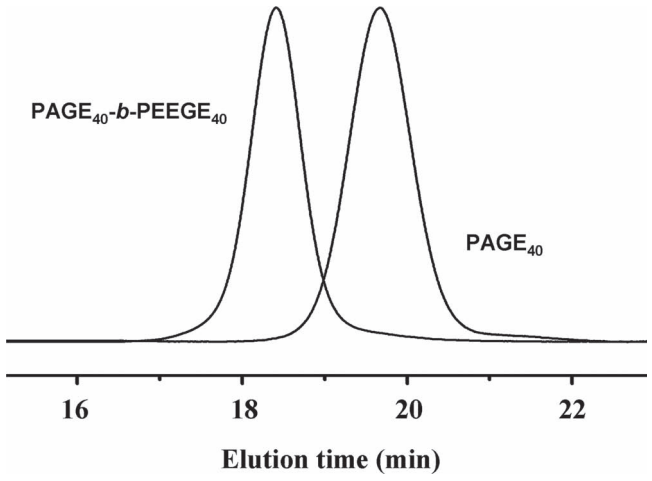

Figure 6. SEC chromatographs of $PAGE_{40}$ homopolymer and $PAGE_{40}$-*b*-$PEEGE_{40}$ diblock copolymer (Table 2, Entry 2).

AGE polymerization in the first step) and the diblock copolymer product (obtained from the EEGE polymerization in the second step). All samples displayed a sharp unimodal peak with a low PDI value (1.11 – 1.13). Similar SEC chromatograms were observed for all diblock copolyether products, regardless of the composition. These results collectively indicate that, with the aid of PPA/*t*-Bu-P_4 catalyst system, sequential anionic ROPs of AGE and EEGE in various feed ratios proceeded successfully in a living manner without side reactions to yield well-defined linear PAGE-*b*-PEEGE diblock copolymers. The results further confirm that in the sequential anionic diblock copolymerization with the PPA/*t*-Bu-P_4 catalyst system, the living alkoxide of the first PAGE block (which was prepared in the first polymerization step) selectively attacked the epoxide ring of the EEGE monomer in the second polymerization step. The resulting chain alkoxide proceeded with nucleophilic attack on the monomer epoxide ring, completely preventing chain transfer reactions.

The obtained linear diblock copolyethers have reactive allyl groups on the PAGE block. The blocks can be selectively deprotected, providing a versatile functional linear aliphatic diblock copolyether platform for a variety of post-reaction modifications appropriate for a particular application. Selective deprotection reactions are shown in Scheme 1. Examples showing the potential of these polymers for further chemical modification and functionalization were also successfully demonstrated.

The ethoxyethyl side groups of the PEEGE blocks in the diblock copolymers were easily cleaved in a mild acidic THF solution with the aid of hydrochloric acid. The side groups thereby converted to the corresponding polyglycidol (PG) block, the hydroxyl groups of which were suitable for further chemical modification. NMR analysis of the PAGE-*b*-PG (**2**) product confirmed that mild hydrochloric acid treatment completely cleaved away the protection groups from the PEEGE block while preserving the PAGE block intact (**Figures 7**a and S3a). The hydroxyl groups in the resulting PG block could not be detected in the NMR spectra in the presence of $CDCl_3$ because of the relatively low solubility of the polymer (Figure 7a); however, the groups were clearly detected in the spectra measured using DMSO-d_6 (Figure S3a, Supporting Information). As an example, the deprotected hydroxyl groups in the resulting PG block of the diblock copolyether were shown to undergo esterification in the presence of *n*-dodecanoic acid, with the aid of EDC and DMAP, yielding a brush block consisting of *n*-alkyl bristles. The degree of esterification was monitored by measuring the integration ratio of the signals at 2.68 ppm (CH_2 of the initiator (Ph−CH_2CH_2CH_2O)) and 2.30 ppm (ester link formation (C(=O)OCH_2)) in the NMR

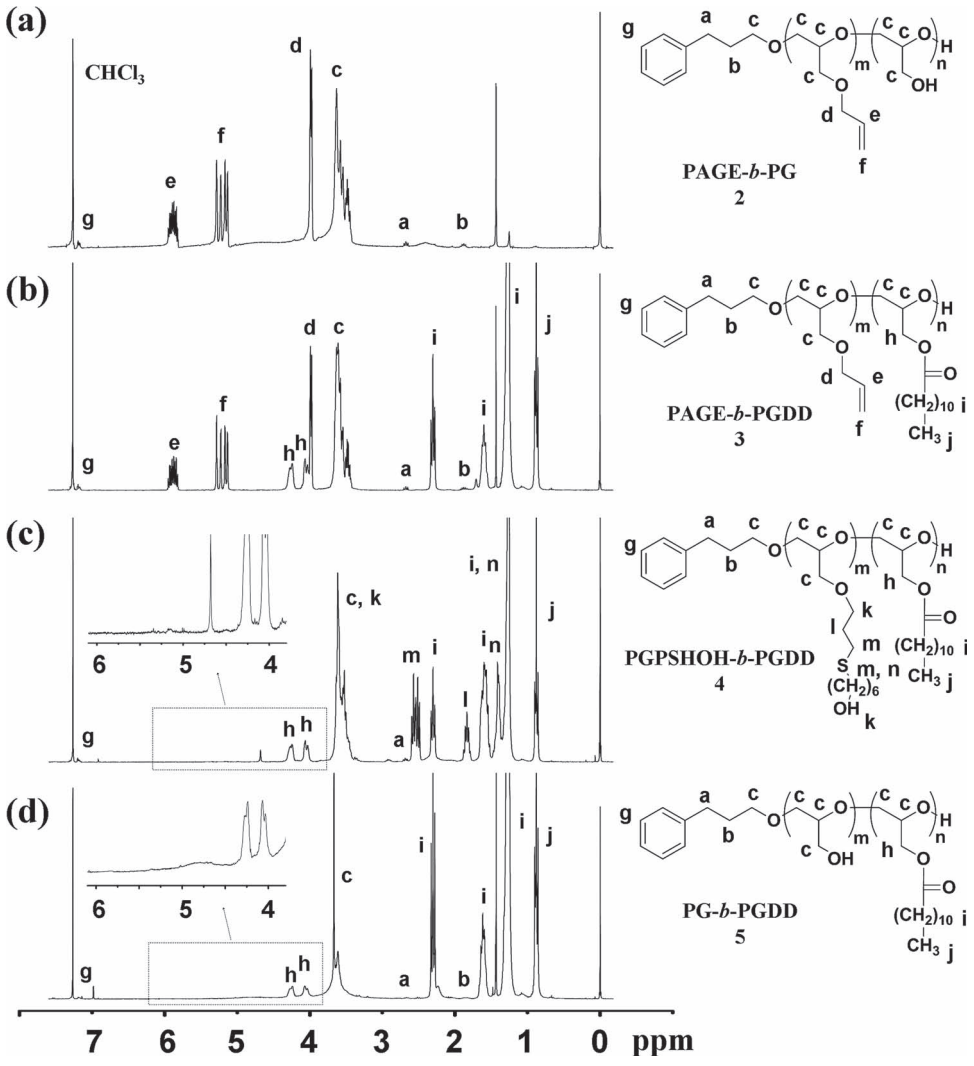

Figure 7. ^{1}H NMR spectra of $PAGE_{40}$-*b*-PG_{40} (**2**), $PAGE_{40}$-*b*-$PGDD_{40}$ (**3**), $PGPSHOH_{40}$-*b*-$PGDD_{40}$ (**4**) and PG_{40}-*b*-$PGDD_{40}$ (**5**) in $CDCl_3$. All of the polymers were derived from $PAGE_{40}$-*b*-$PEEGE_{40}$ (Table 2, Entry 2). Each inset shows the expanded spectrum of the 3.6–6.2 ppm region.

analysis (Figure 7b). This analysis confirmed that the dodecyl groups were incorporated with ≥99.9% yield into the PG block, yielding the product PAGE-*b*-PGDD (**3**).

The PAGE block of the diblock copolymers presented reactive allyl protecting groups and could, therefore, undergo addition reactions. The PAGE block in the diblock copolyether **3** was successfully submitted to an addition reaction with 6-mercapto-1-hexanol to produce the corresponding brush block composed of 1-hydroxyhexylthiopropyl groups as bristles: PGPSHOH-*b*-PGG (**4**). In this reaction, the presence of excess thiol completely prevented undesired cross-linking reactions between the allyl double bonds. The obtained product **4** was characterized by ^{1}H and two-dimensional (2D) ^{1}H–^{13}C NMR spectroscopy (Figure 7c and Figure S4, Supporting Information). The ^{1}H NMR spectrum showed that the characteristic peaks of the allyl groups at 4.0, 5.15, 5.25 and 5.88 ppm completely disappeared while the characteristic peaks of the thioether groups appeared at 1.44, 1.86, 2.54, and 2.60 ppm.

The allyl groups of the PAGE block in the diblock copolymer PAGE-*b*-PGDD (**3**) were also easily cleaved out with the aid of Pd(0)/charcoal and *p*-TsOH to yield the corresponding polyglycidol (PG) block with reactive hydroxyl groups suitable for further functionalization. The obtained product PG-*b*-PGDD (**5**) was amphiphilic, as observed for the polymer **2** and, thus, could be characterized in $CDCl_3$ and DMSO-d_6 by NMR spectroscopy (Figure 7d and Figure S3b, Supporting Information). The NMR analysis found that the allyl groups in the PAGE block were completely cleaved out, but the PGDD block was preserved without any damage.

Thermal properties of the synthesized polyethers and their post-modification products were examined by thermogravimetry (TGA) and differential scanning calorimetry (DSC). The results are summarized in **Table 3**; some representatives of the TGA and DSC thermograms were given in Figures S5 and S6, Supporting Information. Both PAGE and PEEGE homopolymers were found amorphous. PAGE revealed relatively lower

Table 3. Thermal properties of the synthesized linear polyethers (homopolyethers and diblock copolyethers) and their post-modification products.

Polymer	T_d [°C][a)]	T_g [°C][b)]	T_m [°C][c)]
$PAGE_{40}$	339.0	–76.0	
$PEEGE_{40}$	288.0	–64.0	
PG_{80}	323.0	–15.4	
$PGPSHOH_{80}$	336.0	–59.0	
$PGDD_{80}$	318.0	–6.2	32.9
$PAGE_{20}$-*b*-$PEEGE_{60}$	300.0	–76.0 (PAGE), –64.0 (PEEGE)	
$PAGE_{40}$-*b*-$PEEGE_{40}$	323.0	–76.0 (PAGE), –63.0 (PEEGE)	
$PAGE_{60}$-*b*-$PEEGE_{20}$	321.0	–75.0 (PAGE), –64.0 (PEEGE)	
$PAGE_{20}$-*b*-PG_{60}	302.6	–74.0 (PAGE), –28.0 (PG)	
$PAGE_{40}$-*b*-PG_{40}	303.5	–76.0 (PAGE), –28.0 (PG)	
$PAGE_{60}$-*b*-PG_{20}	310.6	–76.0 (PAGE), –28.0 (PG)	
$PAGE_{20}$-*b*-$PGDD_{60}$	334.8	–77.0 (PAGE), –6.9 (PGDD)	23.0
$PAGE_{40}$-*b*-$PGDD_{40}$	338.3	–76.0 (PAGE), –7.4 (PGDD)	21.5
$PAGE_{60}$-*b*-$PGDD_{20}$	300.0	–76 (PAGE), –7.3 (PGDD)	9.1, 15.8
$PGPSHOH_{20}$-*b*-$PGDD_{60}$	341.0	–60.0 (PGPSHOH), –6.8 (PGDD)	24.8
$PGPSHOH_{40}$-*b*-$PGDD_{40}$	338.7	–60.0 (PGPSHOH), –7.3 (PGDD)	25.5
$PGPSHOH_{60}$-*b*-$PGDD_{20}$	336.9	–62.0 (PGPSHOH), –7.4 (PGDD)	17.3
PG_{20}-*b*-$PGDD_{60}$	281.0	–23.0 (PG), –6.6 (PGDD)	14.3
PG_{40}-*b*-$PGDD_{40}$	284.7	–22.0 (PG), –7.2 (PGDD)	12.0
PG_{60}-*b*-$PGDD_{20}$	282.0	–22.0 (PG), –7.3 (PGDD)	10.2

[a)]Decomposition temperature at 5% weight loss, which was measured by TGA analysis; [b)]Glass-transition temperature determined from the onset of the glass transition in DSC analysis; [c)]Melting point determined from the peak maximum of the melting transition in the DSC analysis.

glass transition temperature T_g (–76.0 °C) but higher thermal stability (5 wt% weight loss at 339.0 °C (= T_d^5)), compared to those (T_g = –64.0 °C and T_d^5 = 288.0 °C) of PEEGE. Their deprotected products (namely PG) were also amorphous but exhibited much higher T_g (–15.4 °C) but intermediate T_d^5, compared to those of PAGE and PEEGE. PGPSHOH (which is a functional brush polyether obtained from PAGE by the addition of 6-mercapto-1-hexanol to the allyl groups) was amorphous and revealed T_g = –59.0 °C and T_d^5 = 336.0 °C). PGDD (which is another type of brush polyether obtained from PG by esterification of the hydroxymethylenyl groups with *n*-dodecanoic acid) showed a melting point T_m of 32.9 °C and T_d^5 = 318.0 °C. The T_m observation indicates that PGDD is crystalline. Taking into consideration the amorphous PGE, PEEGE and PG, the PGDD' crystalline nature might be attributed to the ordering of *n*-dodecyl bristles. Due to the crystalline nature, the glass transition of this polymer apparently appeared very weak; its T_g was determined to be –6.2 °C.

The synthesized PAGE-*b*-PEEGE products showed T_d^5 = 300 °C to 323 °C, depending on the diblock compositions. They all showed no melting transition but two glass transitions whose T_g values corresponded to those of the homopolyethers, regardless of the diblock compositions. These results suggest that the diblock copolyethers were amorphous and their block components were phase-separated, giving each block' phase domains. Their post-modification products revealed T_d^5 = 282 °C to 338 °C, depending on the compositions and the chemically modified side groups. These polymers basically showed two T_gs, which corresponded to those of the the diblock compositions. In case of the PGDD-based diblock copolyethers, the glass transition of the PGDD block was very weak due to its crystalline nature. The PGDD block' T_m was found to range in 9.1 °C to 25.5 °C, depending on the block lengths and the other counter blocks. The DSC results collectively indicate that all the diblock copolyethers formed phase-separated domains.

Taking the above DSC results into account, PGPSHOH, PGDD and their diblock copolymers in thin films (70 nm thick) were further investigated by synchrotron grazing incidence small- and wide-angle X-ray scattering (GISAXS and GIWAXS) in order to get their structural information. The representatives of the measured scattering patterns are shown in **Figures 8** and **9**.

The PGPSHOH films revealed only one single broad scattering ring at 13.80° (*d*-spacing = 0.48 nm), which corresponded to the amorphous halo (Figure 8a). This featureless scattering pattern confirmed that PGPSHOH is amorphous. In contrast, the PGDD films showed several scattering peaks along the α_f direction at $2\theta_f = 0°$ (Figure 8b). These spots can be assigned by the {001}, {002}, {003}, {004}, {005}, and {006} diffractions in the order of low to high angle, whose relative scattering vector lengths from the specular reflection position are integer orders of the first peak. The appearance of these scattering spots is an indication of the presence of layered structures stacked normal to the film plane. For the multilayer structure, the thickness of

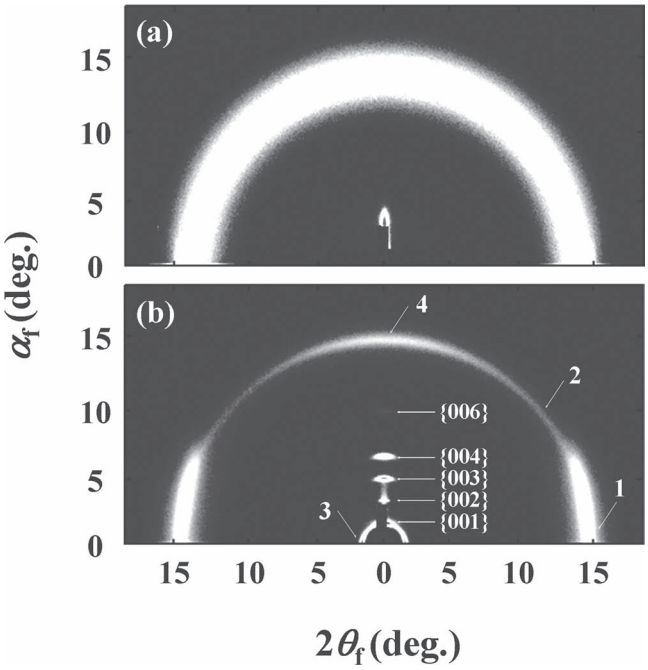

Figure 8. 2D GIWAXS pattern measured with $\alpha_i = 0.110°$ at 20 °C for: PGPSHOH (a) and PGDD (b) thin films (70 nm thick). A synchrotron X-ray source of $\lambda = 0.1155$ nm was used.

each layer (mean long period) was determined to be 3.96 nm from the scattering spots. This layer thickness is very close to twice the length (1.86 nm) of the fully extended bristle; the length of the bristle was estimated using the Cerius^2 software package (Accelrys, San Diego, CA). Beyond the strong spots, a strong anisotropic peak (which is marked by "**1**") appeared at $2\theta_f = 14.66°$ ($\alpha_f = 0°$). Its *d*-spacing value was 0.45 nm. This peak is overlapped in part with a weak ring scattering (which is marked with "**2**"). The weak scattering ring at 13.68° was estimated to have a *d*-spacing of 0.48 nm. This *d*-spacing value is same with that of the amorphous halo ring observed for the PGPSHOH films. Taking this result into account, the strong anisotropic peak **1** is attributed to the mean lateral distance of the bristles aligned normal to the film plane, whereas the ring scattering (13.68°) is caused from the mean interdistance of the polymer backbones. These results collectively indicate that in the thin film the PGDD chains formed multibilayer structure whose individual layers stacked normal to the film plane. The individual layers consist of the polymer backbone chain and two sets of the bristles, where one set of the bristles is linked to the top side of the polymer backbone and another other set is linked to the bottom side of the polymer backbone. The bristles of one layer make no interdigitation with those of the adjacent layer in the stack. In addition, the PGDD films' scattering pattern showed another two peaks (which are marked with "**3**" and "**4**") (Figure 8b). The peak **3** was determined to have a *d*-spacing of 3.96 nm, which was same with that of the first order peak along the α_f direction at $2\theta_f = 0°$, whereas the peak **4** was found to a *d*-spacing of 0.45 nm, which was same with that of the peak **1**. These results indicate that in the film there was also formed a multibilayer structure whose layers stacked along the film plane and, however, its population was much lower than that of the vertically stacked multibilayer structure.

The PGPSHOH and PGDD films were further examined by GISAXS. However, they gave featureless GISAXS patterns, suggesting that no hierarchical structure was formed in both the homopolyether films.

Different from the homopolyethers, their diblock copolymers in thin films were found to show featured GISAXS patterns, confirming that the block components were phase-separated. The PGPSHOH$_{20}$-*b*-PGDD$_{60}$ films revealed a GISAXS pattern (Figure 9A), which resembled that of the hexagonally packed cylinder (HEX) structured poly(styrene-b-isoprene) thin films whose cylinder axes lay along the film plane in the literature.[18] In the scattering pattern, the two spots (A_{T1} at $\alpha_f = 0.23°$ and A_{R1} at $\alpha_f = 0.36°$) along the α_f direction at $2\theta_f = 0.42°$ can be assigned as the diffraction peaks of the {10} plane respectively, whereas another two spots (A_{T2} at $\alpha_f = 0.35°$ and A_{R2} at $\alpha_f = 0.49°$) along the α_f direction at $2\theta_f = 0°$ can be assigned as the diffraction peaks of the {01} plane respectively; here all the designated subscript T and R spots were generated by the transmitted and reflected X-ray beams respectively. From these characteristic spots, the mean interdistance of cylinder layers was estimated to be 14.9 nm and the mean interdistance of the

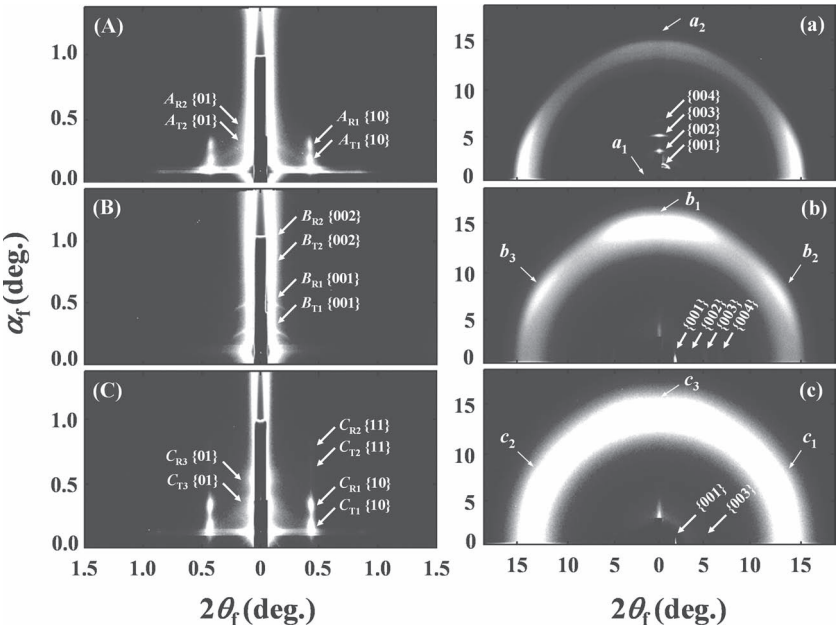

Figure 9. A–C) 2D GISAXS patterns measured with a synchrotron X-ray source of $\lambda = 0.1245$ nm for 70 nm-thick diblock copolyether films: A) PGPSHOH$_{20}$-*b*-PGDD$_{60}$ ($\alpha_i = 0.130°$); B) PGPSHOH$_{40}$-*b*-PGDD$_{40}$ ($\alpha_i = 0.110°$); C) PGPSHOH$_{60}$-*b*-PGDD$_{20}$ ($\alpha_i = 0.150°$). a–c) 2D GIWAXS patterns measured with a synchrotron X-ray source of $\lambda = 0.1155$ nm: a) PGPSHOH$_{20}$-*b*-PGDD$_{60}$ ($\alpha_i = 0.110°$); b) PGPSHOH$_{40}$-*b*-PGDD$_{40}$ ($\alpha_i = 0.120°$); c) PGPSHOH$_{60}$-*b*-PGDD$_{20}$ ($\alpha_i = 0.130°$). All of the measurements were conducted at 20 °C.

cylinders 17.2 nm for the HEX structure. Here the cylinder and matrix phases were composed of the minor PGPSHOH block and the major PGDD block respectively. The HEX-structured PGPSHOH microdomains in the thin films were preferentially oriented with their {10} planes parallel to the film plane. In the GIWAXS pattern, the amorphous PGPSHOH cylinders revealed only weak, broad isotropic ring scattering at 13.80°, whereas the ordered PGDD matrix showed a scattering patter which was similar to that of its homopolymer film (Figure 9a). However, the designated a_1 and a_2 peaks (which were weakly observed in the homopolymer film' GIWAXS pattern) were significantly weakened or not easily discernible. These results indicate that the vertically stacked multibilayer structure was mainly formed in the PGDD matrix; the population of the horizontally stacked multibilayer structure is much less than that in the homopolymer film.

The PGPSHOH$_{40}$-*b*-PGDD$_{40}$ films also revealed a GISAXS pattern, which was quite different from that of the PGPSHOH$_{20}$-*b*-PGDD$_{60}$ films. The films showed several scattering peaks only along the α_f direction at $2\theta_f = 0°$, which were designated by "B_{T1}", "B_{R1}", "B_{T2}", and "B_{R2}" (Figure 9B). These spots can be assigned by the {001} and {002} in the order of low to high angle; the designated subscript T and R spots were generated by the transmitted and reflected X-ray beams respectively. The appearance of these spots indicates that in the polymer films the two blocks underwent phase-separation and formed a lamellar structure whose lamellae stacked along the out-of-plane of the film. From the scattering spots, the mean long period of the lamellar structure was determined to be 16.8 nm. The diblock copolyether films showed a featured GIWAXS pattern (Figure 9b). The weak, broad isotropic amorphous halo ring of the PGPSHOH layers was also observed. However, the PGDD layers exhibited a scattering pattern, which was quite different from those of the homopolymer films and its phases in the PGPSHOH$_{40}$-*b*-PGDD$_{40}$ films. Surprisingly, the {00l} and its higher order reflection spots appeared along the $2\theta_f$ direction at $\alpha_f = 0°$ rather than the α_f direction at $2\theta_f = 0°$. The scattering peak b_1 at $\alpha_f = 14.66°$ ($2\theta_f = 0°$) was significantly enhanced in intensity; in contrast the strong peak at $2\theta_f = 14.66°$ ($\alpha_f = 0°$) (which was observed in the PGDD homopolymer and PGPSHOH$_{20}$-*b*-PGDD$_{60}$ films) completely disappeared. These results collectively indicate that for the vertically stacked lamellar structure in the PGPSHOH$_{40}$-*b*-PGDD$_{40}$ films, the individual PGDD lamellae consisted of a multibilayer structure whose layers stacked along the lamellar plane (i.e., the film plane). The PGDD layers further revealed two additional peaks, which were designated by "b_2" and "b_3". Their *d*-spacing value was same with that (0.45 nm) of the scattering peak b_1. Their location was found to be defined by the azimuthal angle of ca. 30°. These facts suggest that the *n*-dodecyl bristles in the ordered PGDD lamella formed a hexagonal packing.

The PGPSHOH$_{60}$-*b*-PGDD$_{20}$ films also revealed a GISAXS pattern (Figure 9C), which was similar to that of the PGPSHOH$_{20}$-*b*-PGDD$_{60}$ films. However, the PGPSHOH$_{60}$-*b*-PGDD$_{20}$ films showed additionally the two diffraction peaks of the {11} plane, which were designated by "C_{T2}" and "C_{R2}". These results collectively inform that the PGPSHOH$_{60}$-*b*-PGDD$_{20}$ films the two block components were phase-separated, forming a HEX structure whose {10} planes were parallel to the film plane. Moreover, the formed HEX structure had relatively higher ordering, compared to that formed in the PGPSHOH$_{20}$-*b*-PGDD$_{60}$ films. In this diblock copolyether, the PGDD is the minor component. Therefore, the cylinder phase was the PGDD block while the matrix was the PGPSHOH block. The mean interdistance of cylinder layers was estimated to be 14.7 nm and the mean interdistance of the cylinders 16.8 nm. These structural parameters are similar to those of the HEX structure in the PGPSHOH$_{20}$-*b*-PGDD$_{60}$ films; however, their cylinder and matrix phases were inversed each other. The polymer films also showed a GIWAXS pattern similar to that of the PGPSHOH$_{40}$-*b*-PGDD$_{40}$ films (see the peaks c_1, c_2 and c_3, an isotropic amorphous halo ring and some other peaks in Figure 9c). However, the isotropic amorphous halo ring at 13.80° was significantly enhanced in intensity, which was attributed to the major PGPSHOH block as the matrix. The multibilayer structured PGDD cylinder phases showed only the {00l} and {003} diffractions along the $2\theta_f$ direction at $\alpha_f = 0°$. The other high order peaks were not easily discernible, which might result from the relatively small volume of the PGDD block component in the film and also from somewhat lowering of the ordering in the molecular multibilayer structure.

From the above GISAXS and GIWAXS analysis results, nanostructural models are proposed for the PGPSHOH-*b*-PGDD films in three different compositions as shown in **Figures 10**a–c. Molecular packing models are also proposed for the ordered PGDD phases in the phase-separated diblock copolyether films (Figure 10a–c).

Furthermore, the above structural analysis demonstrated that the well-defined linear aliphatic diblock copolyethers (which were synthesized from the AGE and EEGE monomers by a low-temperature metal-free anionic ROP using the PPA/*t*-Bu-P$_4$ catalyst system) are a versatile and selectively functionalizable linear aliphatic polyether platform for a variety of nanostructure constructions and their applications, in addition to various post chemical modifications and applications.

3. Conclusions

We investigated the low-temperature anionic ROPs and copolymerizations of AGE and EEGE monomers with the aid of the PPA/*t*-Bu-P$_4$ catalyst system in an effort to produce well-defined linear glycidol-based homopolyethers and diblock copolyethers, which are versatile and selectively functionalizable aliphatic polyether platforms for a variety of chemical modifications and applications.

Room-temperature metal-free anionic ROP with the PPA/*t*-Bu-P$_4$ catalyst system successfully produced linear PAGE homopolymers with a narrow molecular weight distribution in a manner that was free from side reactions. Low-temperature metal-free anionic polymerization was also useful in the synthesis of linear PEEGE homopolymers; however, this reaction was still accompanied by a small degree of chain transfer side reactions in the early stages of polymerization, which was due to the relatively high acidity of the methylene protons adjacent to the epoxide ring in the monomer.

The chemical properties of the monomers in the context of the anionic homopolymerization reactions were considered in

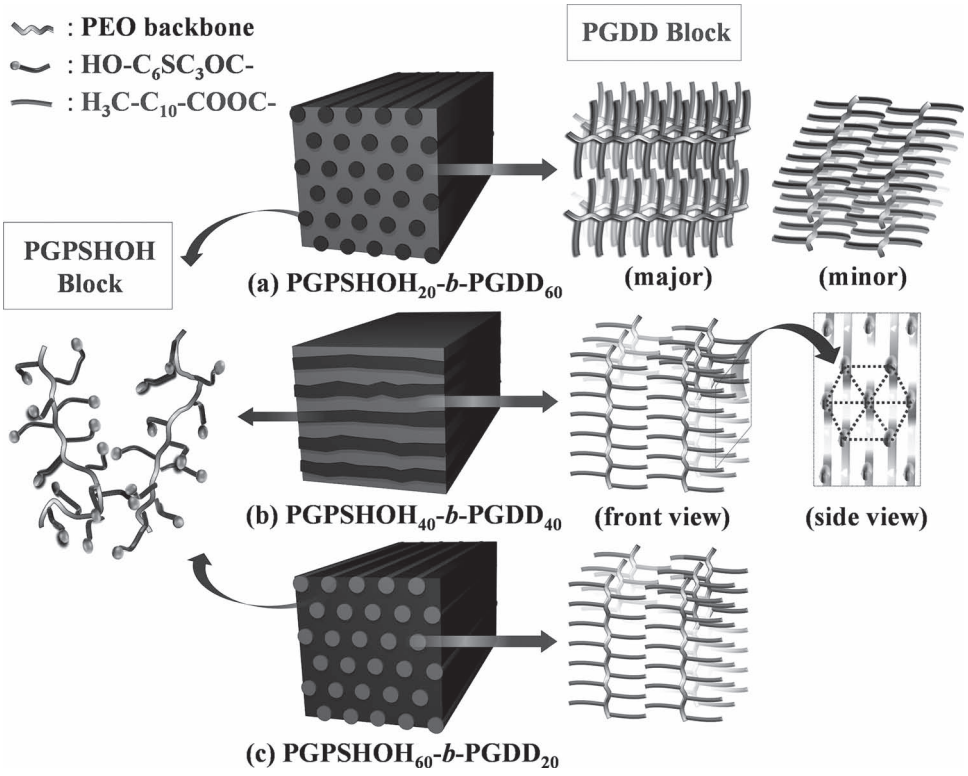

Figure 10. Schematic representations of the nanostructures and molecular packing structures in 70 nm-thick PGPSHOH-*b*-PGDD films proposed from the GIXS (GISAXS and GIWAXS) analysis results: (a) in-plane oriented HEX structure composed of amorphous PGPSHOH cylinders in the ordered PGDD matrix; (b) in-plane oriented lamellar structure composed of amorphous PGPSHOH and ordered PGDD lamellae; (c) in-plane oriented HEX structure consisting of ordered PGDD cylinders in the amorphous PGPSHOH matrix. In all of the cases, the PGDD phase revealed an ordered molecular packing structure, namely a molecular multi-bilayer structure without any interdigitation between the bristles of the adjacent polymer chains; the multi-bilayer structure was preferentially oriented towards a certain direction, depending on the nanostructures.

designing the reaction protocol. AGE and EEGE were fed as the first and second monomers, respectively, in a sequential stepwise manner to achieve room-temperature metal-free anionic polymerization. This approach successfully yielded the well-defined linear diblock copolyether, PAGE-*b*-PEEGE, free from unfavorable side reactions. This polymerization approach further yielded well-defined linear PAGE-*b*-PEEGE polymers with a narrow molecular weight distribution over a wide range of monomer compositions.

The allyl groups in the PAGE block of the obtained linear diblock copolymers were found to selectively react with thiols (for example, 6-mercapto-1-hexanol), demonstrating their availability for post-chemical modification and functionalization. The allyl groups in the PAGE block could be selectively eliminated in a deprotection reaction with the aid of a palladium catalyst system, thereby providing hydroxyl side groups that permitted further chemical modification and functionalization. The ethoxyethyl groups of the PEEGE block could be selectively deprotected under mild acidic conditions to provide hydroxyl side groups for further chemical modification and functionalization. As an example of the post-modification potential, the deprotected hydroxyl groups in the PEEGE block successfully underwent esterification with *n*-dodecanoic acid in 100% yield.

Moreover, the well-defined diblock copolyethers were found to undergo favorably phase-separation and form various nanostructures as well as block-chain conformations and ordering, depending on the bristles incorporated by post-reaction modifications.

Overall, this study demonstrated that a low-temperature metal-free anionic ROP using the PPA/*t*-Bu-P_4 catalyst system is suitable for the production of well-defined linear PAGE homopolymers and their diblock copolymers using EEGE monomer over a range of compositions with the sequential stepwise feeding of AGE and EEGE as the first and second monomers. The diblock copolymers constitute a versatile and selectively functionalizable linear aliphatic polyether platform that is useful for a variety of post-reaction modifications and applications. In particular, the well-defined diblock copolyethers also are a versatile linear aliphatic polymer platform for a variety of selectively functionalized nanostructures and their applications.

4. Experimental Section

Materials: AGE monomer (≥99%, Aldrich) and PPA initiator (98.0%, Aldrich) were distilled over CaH_2 under reduced pressure and stored under nitrogen before use. EEGE monomer was synthesized according to a method reported in the literature,[4] distilled over CaH_2 under reduced pressure and stored under nitrogen before use. *t*-Bu-P_4 promoter (1.0 M solution in hexane, Aldrich) were used as received. Toluene (99.8%, anhydrous, Sigma-Aldrich) and was distilled over sodium benzophenone ketyl before use. Azobisisobutyronitrile (AIBN)

(98%, Acros) was recrystallized from ethanol. *N,N*-Dimethylformamide (DMF) (99.8%, anhydrous, Sigma-Aldrich) was dried over molecular sieve (4 Å). Other chemicals were purchased from Aldrich and used as received: tetrahydrofuran (THF; >99%), dichloromethane (CH_2Cl_2; ≥99.8%), methanol (MeOH; 99.8%), activated alumina, chloroform ($CHCl_3$; >99%), *N*-(3-dimethylaminopropyl)-*N'*-ethylcarbodiimide hydrogenchloride (EDC; ≥98.0%), 4-(dimethylamino)pyridine (DMAP; 99%), hydrochloric acid (HCl; 35%), 6-mecapto-1-hexanol (99%), palladium on charcoal (Pd/C; 10% Pd), and *p*-toluenesulfonic acid monohydrate (*p*-TsOH; ≥98.5%).

Characterization: ^{1}H NMR spectroscopy analysis was carried out using a Bruker AV300 FT-NMR spectrometer at 300 MHz. ^{13}C NMR spectroscopy analysis was conducted using a Bruker AV300 FT-NMR spectrometer at 75 MHz and a Bruker DRX 500 FT-NMR spectrometer at 125 MHz. 2D NMR spectra were recorded on a Bruker AVANCE-III 600 FT-NMR spectrometer, which were operated at 600 MHz for ^{1}H NMR and 150 MHz for ^{13}C NMR. Deuterated chloroform ($CDCl_3$) was used as a solvent; tetramethylsilane was used as an internal standard. Infrared (IR) spectroscopy measurements were conducted using an FT-IR spectrometer (ATI Mattson, Model Research Series 2) equipped with a liquid nitrogen-cooled mercury cadmium telluride (MCT) detector. Molecular weight and PDI were measured at 40 °C using a SEC system (Spectra-series UV 2000 UV/vis adsorption detector, Viscotek TDA 305 light scattering and RI detector) with two mixed-bed columns (Varian, PLgel Mixed-E, 300 × 7.5 mm) calibrated with polystyrene standards; THF was as an eluent and a flow rate of 0.8 mL/min was employed. Mass spectroscopy analysis was also performed using a MALDI-TOF mass spectrometer (Bruker REFLEX-III). All MALDI-TOF mass spectra were recorded by reflective mode with the accelerating potential of 20 kV. Dithranol was employed as a matrix with sodium trifluoroacetate as a cationizing agent and a standard kit (Applied Biosystems, calibration mixture 2) was used for the calibration. TGA and DSC measurements were carried out under a nitrogen atmosphere using a thermogravimeter (model TG/DTA 6200, Seiko Instruments, Japan) and a calorimeter (model DSC 6200, Seiko Instruments, Japan). A rate of 10.0 °C/min was employed for heating and cooling runs. Grazing incidence X-ray scattering (GIXS) measurements were carried out at the 3C and 9A beamlines of the Pohang Light Source II (PLS-II), Pohang Accelerator Laboratory, Pohang University of Science & Technology.[19] Thin polymer film samples were measured at a sample-to-detector distance (SDD) of 131 mm and 2995 mm. Scattering data were typically collected for 2 – 60 s using an X-ray radiation source with a wavelength λ of 0.1155 nm and 0.1245 nm and a 2D charge-coupled detector (CCD) (Roper Scientific, Trenton, NJ, USA). The incidence angle α_i of the X-ray beam was set at 0.110 – 0.150°, which are between the critical angles of the polymer film and the silicon substrate ($\alpha_{c,f}$ and $\alpha_{c,s}$). Scattering angles were corrected according to the positions of the X-ray beams reflected from the silicon substrate with respect to a precalibrated silver behenate powder (TCI, Japan). Aluminum foil pieces were applied as a semi-transparent beam stop because the intensity of the specular reflection from the substrate was much stronger than the scattering intensity of the polymer films near the critical angle. The polyether films were prepared on precleaned silicon substrates by conventional spin-coating and subsequent drying in vacuum at room temperature for 2 days. The polymer solutions were prepared with a concentration of 1.0 wt% in THF and filtered with polytetrafluoroethylene membranes of pore size 0.2 μm. The thicknesses of the polymer films were measured by using a spectroscopic ellipsometer (model M2000, Woollam, USA).

Polymerizations: All anionic polymerizations were conducted in a glovebox equipped with a gas purification system (molecular sieve and copper catalyst) and a dry argon atmosphere. A typical procedure for the polymerizations was as follows. The *t*-Bu-P_4 promoter (34.2 μL as 1.0 M solution, 34.2 μmol) was added to a solution of the PPA initiator (4.66 mg, 34.2 μmol) in toluene (0.456 mL). AGE (0.162 mL, 1.37 mmol) was then added to the initiator/promoter solution. After stirring for 20 h, the polymerization was quenched by the addition of benzoic acid (21 mg). The polymerization mixture was diluted by THF and then passed through activated alumina columns to remove the catalyst residue and excess benzoic acid. After filtration, the filtrate was removed the solvent under vacuum, giving the target polymer product, poly(allyl glycidyl ether) (PAGE). The monomer conversion was determined from the ^{1}H NMR spectroscopy measurements of the polymerization mixture after complete drying of the polymer under vacuum. Yield: 72%. The conversion of AGE by NMR was 99.9%. ^{1}H NMR (300 MHz, $CDCl_3$, δ (ppm)): 7.21–7.29 (m, aromatic protons from initiator), 5.88 (m, 1H, $-OCH_2CHC(H_a)H_b$), 5.25 (d, 1H, $-OCH_2CHC(H_a)H_b$), 5.15 (d, 1H, $-OCH_2CHC(H_a)H_b$), 4.0 (d, 2H, $-OCH_2CHC(H_a)H_b$) 3.43–3.69 (m, $-OCH_2CH$, CH_2 groups directly bonded to the main chain, Ph-$CH_2CH_2CH_2O$), 2.68 (t, 2H, Ph-$CH_2CH_2CH_2O$), 1.87 (m, 2H, Ph-$CH_2CH_2CH_2O$); ^{13}C NMR (75 MHz, $CDCl_3$, δ (ppm)): 31.2 (Ph$-CH_2CH_2CH_2O$), 32.3 (Ph$-CH_2CH_2CH_2O$), 69.8 (CH_2 groups directly bonded to the main chain), 70.0 ($-OCH_2CH-$), 70.6 (Ph$-CH_2CH_2CH_2O$), 72.2 ($-OCH_2CHCH_2$(allyl)), 78.9 ($-OCH_2CH-$), 116.7 ($-OCH2CHCH_2$(allyl)), 125.7, 128.3, 128.4 (aromatic carbons from initiator), 134.9 ($-OCH_2CHCH_2$(allyl)), 141.9(aromatic carbons from initiator).

In the same manner, the homopolymerization of EEGE was conducted, producing poly(ethoxyethyl glycidyl ether) (PEEGE). Yield: 71%. The conversion of EEGE by NMR was 97%. ^{1}H NMR (300 MHz, $CDCl_3$, δ (ppm)): 7.21–7.29 (m, aromatic protons from initiator), 4.69 (q, 1H, $-OCH(CH_3)O-$), 3.43–3.69 (m, $-OCH_2CH$, CH_2 groups directly bonded to the main chain, $-OCH_2CH_3$, Ph-$CH_2CH_2CH_2O$), 2.68 (t, 2H, Ph$-CH_2CH_2CH_2O$), 1.87 (m, 2H, Pη$-CH_2CH_2CH_2O$), 1.29 (d, 3H, $-OCH(CH_3)O-$), 1.20 (t, 3H, $-OCH_2CH_3$); ^{13}C NMR (75 MHz, $CDCl_3$, δ (ppm)): 15.3 ($-OCH_2CH_3$), 19.8 ($-OCH(CH_3)O-$, 31.2 (Ph$-CH_2CH_2CH_2O$), 32.3 (Pη$-CH_2CH_2CH_2O$), 60.7 ($-OCH_2CH_3$), 64.8 (CH_2 groups directly bonded to the main chain), 70.0 ($-OCH_2CH-$), 70.6 (Ph$-CH_2CH_2CH_2O$), 78.9 ($-OCH_2CH-$), 99.7 ($-OCH(CH_3)O-$), 125.7, 128.3, 128.4, 141.9 (aromatic carbons from initiator).

For the block copolymerization, a solution of the second monomer EEGE (0.205 mL, 1.37 mmol) in toluene (0.684 mL) was added after completing of the polymerization of the first monomer, AGE. Here, the completion of the polymerization of the first monomer was confirmed by NMR spectroscopy analysis before adding of the second monomer. After the polymerization of the second monomer for an additional 20 h, the same quenching and purification procedures as used in the homopolymerization were carried out, giving the target diblock copolymer, poly(allyl glycidyl ether-*b*-ethoxyethyl glycidyl ether) (PAGE-*b*-PEEGE) (**1**) (Scheme 1). Yield: 70%. The conversions of AGE and EEGE by NMR were 99.9% and 97%, respectively. ^{1}H NMR (300 MHz, $CDCl_3$, δ (ppm)): 7.21–7.29 (m, aromatic protons from initiator), 5.88 (m, 1H, $-OCH_2CHC(H_a)H_b$), 5.25 (d, 1, $-OCH_2CHC(H_a)H_b$), 5.15 (d, 1H, $-OCH_2CHC(H_a)H_b$), 4.69 (q, 1H, $-OCH(CH_3)O$-$_{EEGE}$), 4.0 (d, 2H, $-OCH_2CHC(H_a)H_b$), 3.43–3.69 (m, $-OCH_2CH$, CH_2 groups directly bonded to the main chain, $-OCH2CH_3$-$_{EEGE}$, Ph-$CH_2CH_2CH_2O$), 2.68 (t, 2H, Ph$-CH_2CH_2CH_2O$), 1.87 (m, 2H, Ph$-CH_2CH_2CH_2O$), 1.29 (d, 3H, $-OCH(CH_3)O$-$_{EEGE}$), 1.20 (t, 3H, $-OCH_2CH_3$-$_{EEGE}$); ^{13}C NMR (75 MHz, $CDCl_3$, δ): 15.3, 19.8, 31.2, 32.3, 60.7, 64.8, 69.8, 70.0, 70.6, 72.2, 78.9, 99.7, 116.7, 125.7, 128.3, 128.4, 134.9, 141.9; IR (film, ν (cm^{-1})): 3100 (w), 2978 (s), 2930–2870 (s), 1650 (w), 1455 (m), 1380, 1340, 1300, 1270 (m), 1135–1060 (s), 1000 (m), 930 (m), 877 (m) (Figure S7, Supporting Information).

Deprotections and Functionalizations: For the diblock copolymers synthesized above, each block can be deprotected and further functionalized in various ways. Typical procedures for deprotections of the allyl and ethoxyethyl groups were as follows. And, examples for the functionaliztion of the deprotected glycidol blocks were given here. First, the exthoxyethyl groups in the PEEGE block were selectively deprotected in a mild acidic condition, in accordance to a method reported in the literature,[8] and then functionalized. A PAGE-*b*-PEEGE diblock copolymer (1.80 g, EEGE = 6.90 mmol: entry 2 in Table 2) was dissolved in THF (18 mL). Hydrochloric acid (6.90 mmol, 1 equiv.) was added and stirred at room temperature for 5 h. Then, the reaction solution was neutralized by sodium bicarbonate and the solvent was removed under reduced pressure. The product was dissolved in $CHCl_3$ and the salts were filtered out. The remaining $CHCl_3$ was removed under reduced pressure and dried under vacuum, giving the target product poly(allyl glycidyl ether-*b*-

gylcidol) (PAGE-*b*-PG) (**2**) (Scheme 1). Yield: 87%. ^{1}H NMR (300 MHz, DMSO-d_6, δ (ppm)): 7.16-7.29 (m, 5H, aromatic protons from initiator), 5.88 (m, 35H, $-OCH_2CHC(H_a)H_b$), 5.25 (d, 35H, $-OCH_2CHC(H_a)H_b$), 5.15 (d, 35H, $-OCH_2CHC(H_a)H_b$), 4.50 (br, 37H, $-(CH_2)OH$), 4.00 (d, 70H, $-OCH_2CHC(H_a)H_b$), 3.43-3.69 (m, $-OCH_2CH$, CH_2 groups directly bonded to the main chain, $Ph-CH_2CH_2CH_2O$), 2.68 (t, 2H, $Ph-CH_2CH_2CH_2O$), 1.80 (m, 2H, $Ph-CH_2CH_2CH_2O$).

The obtained product **2** (1.13 g, PG = 5.98 mmol) were dissolved in anhydrous $CHCl_3$ (43mL) with *n*-dodecanoic acid (1.439 g, 7.18 mmol, 1.2 equiv.), EDC (1.38 g, 7.18 mmol) and DMAP (0.44 g, 3.59 mmol) and stirred at 30 °C for 24 h. Then, the solvent was removed under reduced pressure. The residue was purified by column chromatography on silica gel with a $CHCl_3$ as the eluent and concentrated under reduced pressure, giving the target polymer poly(allyl glycidyl ether-*b*-gylcidyl dodecanoate) (PAGE-*b*-PGDD) (**3**) (Scheme 1). Yield: 74.0%. ^{1}H NMR (300 MHz, $CDCl_3$, δ (ppm)): 7.21-7.29 (m, 5H, aromatic protons from initiator), 5.88 (m, 40H, $-OCH_2CHC(H_a)H_b$), 5.25 (d, 40H, $-OCH_2CHC(H_a)H_b$), 5.15 (d, 41H, $-OCH_2CHC(H_a)H_b$), 4.25, 4.06 (br, 84H, $CH_{2\text{-GDD}}$ groups directly bonded to the main chain), 4.0 (d, 81H, $-OCH_2CHC(H_a)H_b$), 3.43–3.69 (m, 340H, $-OCH_2CH$, $CH_{2\text{-AGE}}$ groups directly bonded to the main chain, $Ph-CH_2CH_2CH_2O$), 2.68 (t, 2H, $Ph-CH_2CH_2CH_2O$), 2.30 (t, 90H, $-COOCH_2CH_2(CH_2)_8$-), 1.87 (m, 2H, $Ph-CH_2CH_2CH_2O$), 1.60 (br, 90H, $-COOCH_2CH_2(CH_2)_8$), 1.27 (br, 720H, $-(CH_2)_8CH_3$), 0.88 (t, 135H, $-(CH_2)_8CH_3$); ^{13}C NMR (75 MHz, $CDCl_3$, δ (ppm)): 14.1 ($-(CH_2)_8CH_3$), 22.7 ($-(CH_2)_7CH_2CH_3$), 26.9 ($-COOCH_2CH_2(CH_2)_8$), 29.4, 29.5, 29.7, 29.9, 30.3 ($-(CH_2)_6(CH_2)_2CH_3$), 31.9 ($-CH_2CH_2CH_3$), 41.2 ($-COOCH_2$), 63.3 ($CH_{2\text{-GDD}}$ groups directly bonded to the main chain), 69.8 ($CH_{2\text{-AGE}}$ groups directly bonded to the main chain), 70.0 ($-OCH_2CH-$), 72.2 ($-OCH_2CHCH_2$(allyl)), 78.8 ($-OCH_2CH-$), 116.7 ($-OCH_2CHCH_2$(allyl)), 134.9 ($-OCH_2CHCH_2$(allyl)), 173.3 ($-COOCH_2CH_2(CH_2)_8$).

Second, the allyl groups in the PAGE block were either functionalized or deprotected for further modifications. The product **3** (1.64 g, AGE = 4.31 mmol) was dissolved in a mixture (27 mL) of anhydrous $CHCl_3$ and DMF (1:3 in volume) and placed in Schlenk flask. AIBN (0.53 g, 3.23 mmol, 0.75 equiv.) and 6-mercapto-1-hexanol (4.72 mL, 34.5 mmol, 8 equiv.) were added to the polymer solution and then degassed by three freeze-pump-thaw cycles. The solution was stirred at 75 °C for 24 h and then cooled to room temperature. The solvent was removed by vacuum distillation. The concentrated polymer solution was poured into a mixture of deionized water and methanol (1:1.5 in volume) and precipitated several times from CH_2Cl_2 into methanol. The polymer product poly(hydroxyhexylthiopropyl glycidyl ether-*b*-glycidyl dodecanoate) (PGPSHOH-*b*-PGDD) (**4**) (Scheme 1) was filtered and dried at room temperature under vacuum. Yield: 71%. ^{1}H NMR (300 MHz, $CDCl_3$, δ (ppm)): 7.21-7.29 (m, aromatic protons from initiator), 4.25, 4.06 (br, 2H, $CH_{2\text{-GDD}}$ groups directly bonded to the main chain), 3.43–3.69 (m, $-OCH_2CH$, $CH_{2\text{-GPSHOH}}$ groups directly bonded to the main chain, $-OCH_2CH_2CH_2S-$, $-CH_2CH_2OH$, $Ph-CH_2CH_2CH_2O$), 2.68 (t, $Ph-CH_2CH_2CH_2O$), 2.60, 2.54 (m, 4H, $-CH_2CH_2SCH_2$), 2.30 (t, 2H, $-COOCH_2CH_2(CH_2)_8$), 1.87 (m, $Ph-CH_2CH_2CH_2O$), 1.86 (t, 2H, $-OCH_2CH_2CH_2S-$), 1.59-1.63 (br, 6H, $-SCH_2CH_2(CH_2)_3$, $-CH_2CH_2OH$, $-COOCH_2CH_2(CH_2)_8$), 1.44 (br, 4H, $-S(CH_2)_2(CH_2)_2(CH_2)_2OH-$), 1.27 (br, 16H, $-(CH_2)_8CH_3$), 0.88 (t, 3H, $-(CH_2)_8CH_3$); ^{13}C NMR (75 MHz, $CDCl_3$, δ (ppm)): 14.1 ($-(CH_2)_8CH_3$), 22.7 ($-(CH_2)_7CH_2CH_3$), 24.9 ($-COOCH_2CH_2(CH_2)_8$), 25.4 ($-S(CH_2)_3CH_2$), 28.6 ($-S(CH_2)_2CH_2$), 28.8 ($-CH_2SCH_2$), 29.2, 29.3, 29.5, 29.6, 29.64 ($-(CH_2)_6(CH_2)_2CH_3$), 29.7 ($-SCH_2CH_2(CH_2)_3$), 29.9 ($-OCH_2CH_2CH_2S-$), 31.9 ($-CH_2CH_2CH_3$), 32.1 ($-CH_2SCH_2$), 32.6 ($-CH_2CH_2OH$), 34.1 ($-COOCH_2$), 62.6 ($-CH_2CH_2OH$), 63.3 ($CH_{2\text{-GDD}}$ groups directly bonded to the main chain), 69.3 ($-OCH_2CH_2CH_2S-$), 69.5–70.0 ($-OCH_2CH-$), 71.1 ($CH_{2\text{-GPSHOH}}$ groups directly bonded to the main chain), 77.7 ($-OCH_2CH-$), 78.8 ($-OCH_2CH-$), 173.3 ($-COOCH_2CH_2(CH_2)_8$).

The allyl groups in the PAGE block were attempted to be cleaved using a system of Pd(0)/charcoal and *p*-TsOH reported in the literature.[14,20] The polymer **3** (1.64 g, AGE = 4.31 mmol) was dissolved in a mixture (8.62 mL) of anhydrous CH_2Cl_2 and methanol (1:1 in volume) and placed in Schlenk flask. The solution was degassed by three freeze-pump-thaw cycles. Pd(0)/C (10% Pd, 0.14 g, 0.13 mmol) and *p*-TsOH (0.82 g, 0.43 mmol) was added to the reaction mixture. The solution was stirred for 4 days and filtered over neutral alumina. The filtrate was dried over sodium carbonate and the solvent was removed by vacuum distillation, giving the target product poly(gycidol-*b*-glycidyl dodecanoate) (PG-*b*-PGDD) (**5**) (Scheme 1). ^{1}H NMR (300 MHz, $CDCl_3$, δ (ppm)): 7.21–7.29 (m, aromatic protons from initiator), 4.25, 4.06 (br, 50H, $CH_{2\text{-GDD}}$ groups directly bonded to the main chain), 3.43–3.69 (m, $2OCH_2CH$, CH_{2-PG} groups directly bonded to the main chain, $Ph2CH_2CH_2CH_2O$), 2.68 (t, $Ph2CH_2CH_2CH_2O$), 2.30 (t, 94H, $2COOCH_2CH_2(CH_2)_8$), 1.87 (m, $Ph2CH_2CH_2CH_2O$), 1.60 (br, 93H, $2COOCH_2CH_2(CH_2)_8$), 1.27 (br, 756H, $2(CH_2)_8CH_3$), 0.88 (t, 141H, $2(CH_2)_8CH_3$); ^{13}C NMR (75 MHz, $CDCl_3$, δ (ppm)): 14.1 ($2(CH_2)_8CH_3$), 22.7 ($2(CH_2)_7CH_2CH_3$), 24.9 ($2COOCH_2CH_2(CH_2)_8$), 29.2, 29.3, 29.4, 29.5, 29.6, 29.64 ($2(CH_2)_6(CH_2)_2CH_3$), 31.9 ($2CH_2CH_2CH_3$), 34.1 ($2COOCH_2$), 63.3 (CH_{2-GDD} groups directly bonded to the main chain), 69.5–70.0 ($2OCH_2CH2$), 79.0 ($2OCH_2CH2$), 174.3 ($2COOCH_2CH_2(CH_2)_8$). Because of the low solubility, the intensities of the hydrophilic parts were very weak.

Supporting Information

Supporting Information is available from the Wiley Online Library or from the author.

Acknowledgements

W.K., Y.R., and K.K. contributed equally to this work. This study was supported by the National Research Foundation (NRF) of Korea (Doyak Program 2011-0028678, Center for Electro-Photo Behaviors in Advanced Molecular Systems (2010-0001784) and Basic Research Grant No. 2010-0023396)) and the Ministry of Education, Science and Technology (MEST) (World Class University Programs (R31-2008-000-10059-0) and BK21 Program). This work was also supported by the Global COE Program (Catalysis as the Basis for Innovation in Materials Science) of the Ministry of Education, Culture, Sports, Science and Technology, Japan. Synchrotron GIXS measurements at the Pohang Accelerator Laboratory were supported by the MEST of Korea, the POSCO company, and the POSTECH Foundation.

Received: April 20, 2012
Revised: June 22, 2012
Published online: July 27, 2012

[1] a) S. Zalipsky, *Bioconjugate Chem.* **1995**, *6*, 150; b) Y. Kodera, A. Matsushima, M. Hiroto, H. Nishimura, A. Ishii, T. Ueno, Y. Inada, *Prog. Polym. Sci.* **1998**, *23*, 1233; c) P. Caliceti, F. M. Veronese, *Adv. Drug Delivery Rev.* **2003**, *55*, 1261.

[2] a) G. Kim, S. Park, J. Jung, K. Heo, J. Yoon, H. Kim, I. J. Kim, J. R. Kim, J. I. Lee, M. Ree, *Adv. Funct. Mater.* **2009**, *19*, 1631; b) G. Kim, Y. Rho, S. Park, H. Kim, S. Son, H. Kim, I. J. Kim, J. R. Kim, W. J. Kim, M. Ree, *Biomaterials* **2010**, *31*, 3816; c) J. C. Kim, J. Jung, Y. Rho, M. Kim, W. Kwon, H. Kim, I. J. Kim, J. R. Kim, M. Ree, *Biomacromolecules* **2011**, *12*, 2822.

[3] a) A. Haouet, M. Sepulchre, N. Spassky, *Eur. Polym. J.* **1983**, *19*, 1089; b) P. Dimitrov, E. Hasan, S. Rangelov, B. Trzebicka, A. Dworak, C. B. Tsvetanov, *Polymer* **2002**, *43*, 7171; c) S. Rangelov, B. Trzebicka, M. Jamroz-Piegza, A. Dworak, *J. Phys. Chem. B* **2007**, *111*, 11127.

[4] a) A. O. Fitton, J. Hill, D. E. Jane, R. Millar, *Synthesis* **1987**, 1140; b) A. Dworak, I. Panchev, B. Trzebicka, W. Walach, *Polym. Bull.* **1998**, *40*, 461.

[5] M. Backes, L. Messager, A. Mourran, H. Keul, M. Moeller, *Macromolecules* **2010**, *43*, 3238.

[6] S. Park, D. Y. Ryu, J. K. Kim, M. Ree, T. Chang, *Polymer* **2008**, *49*, 2170.
[7] a) R. T. Liggins, H. M. Burt, *Adv. Drug Delivery Rev.* **2002**, *54*, 191; b) R. T. Liggins, H. M. Burt, *Int. J. Pharm.* **2001**, *222*, 19.
[8] M. Hans, P. Gasteier, H. Keul, M. Moeller, *Macromolecules* **2006**, *39*, 3184.
[9] a) D. Taton, A. Le Borgne, M. Sepulchre, N. Spassky, *Macromol. Chem. Phys.* **1994**, *195*, 139; b) A. Dworak, I. Panchev, B. Trzebicka, W. Walach, *Macromol. Symp.* **2000**, *153*, 233; c) J.-S. Kim, H.-C. Kim, B. Lee, M. Ree, *Polymer* **2005**, *46*, 7394.
[10] B. F. Lee, M. J. Kade, J. A. Chute, N. Gupta, L. M. Campos, G. H. Fredrickson, E. J. Kramer, N. A. Lynd, C. J. Hawker, *J. Polym. Sci.: Polym. Chem.* **2011**, *49*, 4498.
[11] M. Hans, H. Keul, M. Moeller, *Polymer* **2009**, *50*, 1103.
[12] J. Allgaier, S. Willbold, T. H. Chang, *Macromolecules* **2007**, *40*, 518.
[13] O. Rexin, R. Mülhaupt, *Macromol. Chem. Phys.* **2003**, *204*, 1102.
[14] M. Erberich, H. Keul, M. Moller, *Macromolecules* **2007**, *40*, 3070.
[15] B. Obermeier, H. Frey, *Bioconjugate Chem.* **2011**, *22*, 436.
[16] A. Sunder, H. Türk, R. Haag, H. Frey, *Macromolecules* **2000**, *33*, 7682.
[17] a) H. Schlaad, H. Kukula, J. Rudloff, I. Below, *Macromolecules* **2001**, *34*, 4302; b) B. Eßwein, M. Möller, *Angew. Chem. Int. Ed.* **1996**, *35*, 623; c) B. Eßwein, A. Molenberg, M. Möller, *Macromol. Symp.* **1996**, *107*, 331; d) B. Eßwein, N. M. Steidl, M. Möller, *Macromol. Rapid Commun.* **1996**, *17*, 143; e) H. Misaka, R. Sakai, T. Satoh, T. Kakuchi, *Macromolecules* **2011**, *44*, 9099; f) H. Misaka, E. Tamura, K. Makiguchi, K. Kamoshida, R. Sakai, T. Satoh, T. Kakuchi, *J. Polym. Sci.: Part A: Polym. Chem.* **2012**, *50*, 1941.
[18] a) B. Lee, I. Park, J. Yoon, S. Park, J. Kim, K.-W. Kim, T. Chang, M. Ree, *Macromolecules* **2005**, *38*, 4311; b) M. Ree, D. M. Kim, J. Jung, Y. Rho, B. Ahn, S. Jin, M. Kim, in *Polymer Science: A Comprehensive Reference*, (Eds: K. Matyjaszewski, M. Möller), Elsevier, Amsterdam **2012**, pp. 211–231.
[19] a) J. Yoon, K.-W. Kim, J. Kim, K. Heo, K. S. Jin, S. Jin, T. J. Shin, B. Lee, Y. Rho, B. Ahn, M. Ree, *Macromol. Res.* **2008**, *16*, 575; b) J. Bolze, J. Kim, J.-Y. Huang, S. Rah, H. S. Youn, B. Lee, T. J. Shin, M. Ree, *Macromol. Res.* **2002**, *10*, 2; c) B. Lee, Y.-H. Park, Y. Hwang, W. Oh, J. Yoon, M. Ree, *Nat. Mater.* **2005**, *4*, 147; d) B. Lee, W. Oh, Y. Hwang, Y.-H. Park, J. Yoon, K. S. Jin, K. Heo, J. Kim, K.-W. Kim, M. Ree, *Adv. Mater.* **2005**, *17*, 696; e) B. Ahn, T. Hirai, S. Jin, Y. Rho, K.-W. Kim, M.-a. Kakimoto, P. Gopalan, T. Hayakawa, M. Ree, *Macromolecules* **2010**, *43*, 10568; f) S. Jin, T. Hirai, B. Ahn, Y. Rho, K.-W. Kim, M.-a. Kakimoto, P. Gopalan, T. Hayakawa, M. Ree, *J. Phys. Chem. B* **2010**, *114*, 8033; g) J. Jung, J. C. Kim, Y. Rho, M. Kim, H. Kim, M. Ree, *ACS Appl. Mater. Interfaces* **2011**, *3*, 2655; h) W. Kwon, B. Ahn, D. M. Kim, Y.-G. Ko, S. G. Hahm, Y. Kim, H. Kim, M. Ree, *J. Phys. Chem. C* **2011**, *115*, 19355; i) Y.-G. Ko, W. Kwon, H.-J. Yen, C.-W. Chang, D. M. Kim, K. Kim, S. G. Hahm, T. J. Lee, G.-S. Liou, M. Ree, *Macromolecules* **2012**, *45*, 3749; j) Y.-G. Ko, W. Kwon, D. M. Kim, Y.-S. Gal, M. Ree, *Polym. Chem.* **2012**, *3*, 2028.
[20] J. F. G. A. Jansen, A. A. Dias, M. Dorschu, B. Coussens, *Macromolecules* **2003**, *36*, 3861.